Photogalvanic effect in porphyrin-pyrrolo[3′,4′:1,9]-(C_{60}-I_h)[5,6]fullerene-2′,5′-dicarboxylate systems*

D. V. Androsov, A. A. Strelnikov, A. S. Konev,★ D. A. Lukyanov, A. V. Kazakova, O. V. Levin, and A. F. Khlebnikov

Saint Petersburg State University, Institute of Chemistry,
7-9 Universitetskaya nab., 199034 Saint Petersburg, Russian Federation.
Fax: +7 (812) 363 6722. E-mail: a.konev@spbu.ru

The influence of molecular structural factors of covalently bound porphyrin-fullerene dyads and porphyrin—fullerene binary mixtures on photocurrent in model photoelectrochemical cells was studied. It was found that the photocurrent increased either by introducing solubilizing alkyl groups into the donor (porphyrin) or acceptor (fullerene) fragments, or by covalent binding porphyrin and fullerene into a donor-acceptor dyad.

Key words: fullerenes, porphyrins, photogalvanic effect.

Solar to electrical energy converters based on organic materials are a promising alternative to similar devices made of inorganic semiconductors, due to the possibility of their application onto flexible polymeric carriers by inkjet printing, their low weight, as well as potentially low production costs.[1,2] The active layer of these devices includes electron-donating and electron-withdrawing components, the interaction of which facilitates the dissociation of an exciton (a bound electron—hole pair) into positive and negative charge carriers and their transport to the corresponding electrodes.[2] At the present time, polymer solar cells based on poly-3-hexylthiophene (P3HT), used as a light-absorbing donor component, and substituted methanofullerene (methyl [6,6]-phenyl-C_{61}-butyrate ($PC_{61}BM$)), used as an acceptor component, are the most thoroughly studied.[3] Since the maximum power conversion efficiency (PCE) for solar cells based on P3HT—$PC_{61}BM$ mixtures is 6.5%,[3,4] the search for new photoactive organic materials is continuously underway. In addition to $PC_{61}BM$ and $PC_{71}BM$,[5,6] other fullerene[7] and non-fullerene[8] compounds are used as the acceptor phase. Alongside with conducting polymers alternative to P3HT,[2,8—12] oligomeric and low-molecular-weight organic compounds with an extended π-system,[9,13] which can successfully compete with polymeric materials, are being studied.[1] In particular, a recently published review[13] notes that porphyrin systems both in combination with a thiophene fragment (PCE up to 8.6%), and without it (PCE up to 4.2%) are promising.

One of the important factors affecting the efficiency of organic bulk-heterojunction (BHJ) solar cells is the morphology of the active layer.[1] In order to achieve efficient conversion of absorbed photons into dissociated charge carrier pairs and their complete transfer to the collecting electrodes, it is necessary to ensure the interpenetration of donor and acceptor phases at the nanoscale level with the donor and acceptor domain diameters of 10—20 nm, because in this case the exciton mean free path is comparable with the domain size.[1,2] A good illustration of this principle is the work,[14] which demonstrated that the PCE of photovoltaic cells with a homogeneous active layer based on a covalently bound tetrabenzoporphyrin—$PC_{61}BM$ dyad, providing the highest degree of mixing of donor and acceptor components, is an order of magnitude higher than the efficiency of a cell based on a heterogeneous equimolar tetrabenzoporphyrin—$PC_{61}BM$ mixture.

According to the review,[1] the ideal morphology of the active layer is achieved by organizing the donor and the acceptor components into column-like structures, which facilitate the rapid transport of charges through the donor and the acceptor phase. The possibility of organizing such structures with double channels for charge transport was theoretically predicted for rigid porphyrin-pyrrolofullerene dyads by density functional theory quantum chemical calculations.[15] In our recent work,[16] we synthesized a dyad analogous to the one theoretically investigated in the work,[15] and demonstrated its ability to convert light energy into electric power.

Taking into account the variety of factors which affect the efficiency of the conversion of light energy into electric power, in the present work we search for promising donor—acceptor pairs using the photogalvanic effect of these pairs, assuming that there is a correlation between the magnitude of this effect and the efficiency of charge separation in the photoactive layer of photovoltaic devices based on this donor—acceptor pair. In accordance with

---

* Based on the materials of the V All-Russian Organic Chemistry Conference (ROCC-V) (September 10—14, 2018, Vladikavkaz, Russia).

Published in Russian in *Izvestiya Akademii Nauk. Seriya Khimicheskaya,* No. 4, pp. 0825—0831, April, 2019.

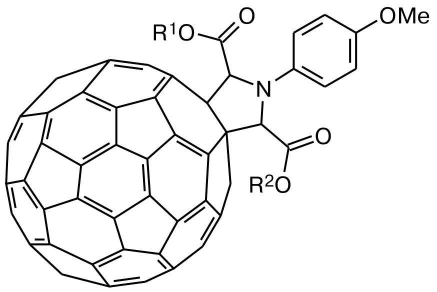

F1—6

Fullerene	R^1	R^2	Configuration
F1	Et	Et	*trans*
F2	Bu	Et	*trans*
F3	Bu	Et	*cis*
F4	Bu	Bu	*trans*
F5	Bu	Bu	*cis*
F6	C_8H_{17}	Et	*trans*

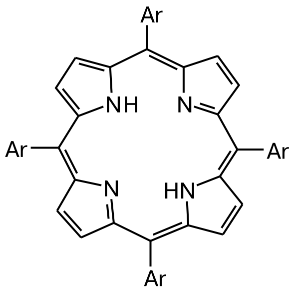

P1—5

Porphyrin	Ar
P1	Ph
P2	4-MeC_6H_4
P3	4-C$F_3C_6H_4$
P4	4-MeOC_6H_4
P5	4-BrC_6H_4

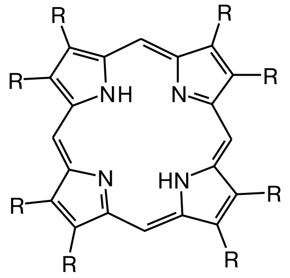

P6, P7

R + R = —$(CH_2)_4$— (**P6**); R = Et (**P7**)

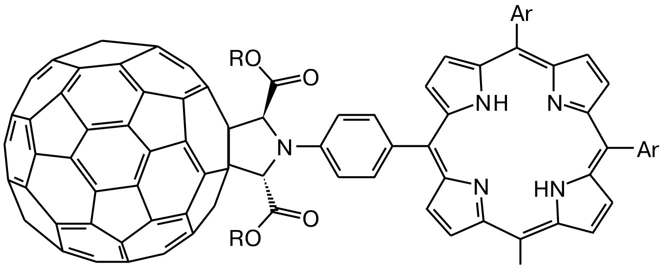

FP1—6

Dyad	R	Ar
FP1	Et	Ph
FP2	Et	4-MeC_6H_4
FP3	Et	4-C$F_3C_6H_4$
FP4	Et	4-MeOC_6H_4
FP5	Et	4-BrC_6H_4
FP6	Bu	4-MeC_6H_4

Fig. 1. Fullerenes (**F**), porphyrins (**P**), and porphyrin-fullerene dyads (**FP**) studied in this work.

this hypothesis, the goal of this work is to study the influence of molecular structural factors in porphyrin-fullerene dyads and porphyrin—fullerene binary mixtures (Fig. 1) on the magnitude of the photogalvanic effect of a model cell in order to search for the most promising candidates for a future development of a bulk heterojunction in organic photovoltaic devices.

Results and Discussion

The photocurrent observed in a photovoltaic cell upon irradiation with a LED (λ_{max} = 470 nm) at an applied potential of 0.1 V was used to characterize the ability of porphyrin-fullerene dyads and porphyrin—fullerene binary mixtures (see Fig. 1) to convert solar energy. The cell, similar to the one described in the work,[17] included a working electrode composed of a test object applied on an indium-tin oxide (ITO) coated glass and ascorbic acid used as an electron transfer mediator. The applied potential of 0.1 V corresponded to the onset of the oxidation of ascorbic acid. Thus, the observed photocurrent corresponds to an increase in the rate of this redox reaction, demonstrating the photocatalytic properties of this porphyrin-fullerene system.

Porphyrin-fullerene dyads **FP1—6** are electrochemically inert at an applied potential of 0.1 V. In a wider range of potentials (−2.0—1.25 V), the dyads exhibit electrochemical behavior typical of porphyrins and pyrrolofullerenes: up to three peaks of reversible reduction are observed in the region of negative potentials (−0.9÷−1.6 V), and one reversible oxidation peak is observed in the region of positive potentials (0.8—1.0 V). A comparison of cyclic voltammograms (CV) of dyads **FP1—5** with CV of model porphyrins **P1—5** and pyrrolofullerene **F1** (Table 1, Fig. 2) shows that the oxidation peak in the region of positive potentials (0.8—1.0 V) corresponds to the oxidation of the

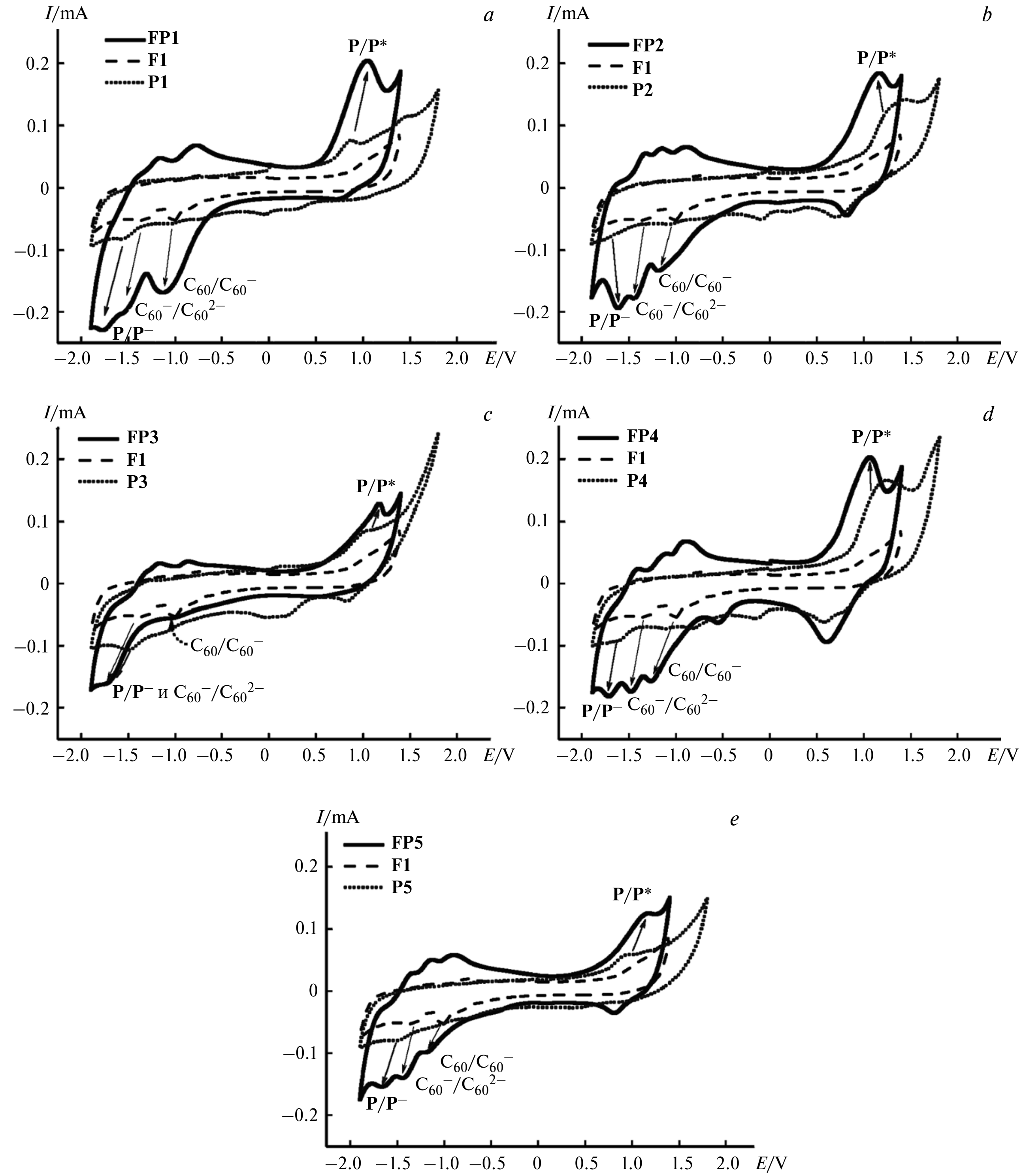

Fig. 2. The CV curves of dyads **FP1—5** compared to the CV curves of pyrrolofullerene **F1** and porphyrins **P1—5**. The CV curves were recorded in thin films on glassy carbon in a 0.1 *M* solution of $LiClO_4$ in MeCN at a potential scan rate of 500 mV s^{-1}.

porphyrin fragment, while the reduction peaks in the region of negative potentials correspond to one- (–0.9÷–1.0 V) and two-electron (–1.3÷–1.4 V) reduction of the fullerene fragment and one-electron reduction of the porphyrin fragment (–1.5÷–1.6 V). As expected, the oxidation potential of the porphyrin fragment in the dyads **FP1**, **FP3—5** and porphyrins **P1**, **P3—5** decreases with increasing donor character of the substituent at *meso*-position of the por-

Table 1. Redox potentials of dyads **FP1—5** compared to the redox potentials of porphyrins **P1—5** and pyrrolofullerene **F1**

Compound	$E_{1/2}$/V				
	$E_{1/2}^{\mathrm{Ox1}}$	$E_{1/2}^{\mathrm{Ox2}}$	$-E_{1/2}^{\mathrm{Red1}}$	$-E_{1/2}^{\mathrm{Red2}}$	$-E_{1/2}^{\mathrm{Red3}}$
FP1	0.88	—	0.96	1.35	1.59
FP2	0.98	—	1.04	1.30	1.47
FP3	1.03	—	0.97	1.46[a]	1.53
FP4	0.83	—	1.08	1.29	1.57
FP5	1.00	—	1.05	1.29	1.50
F1	—	—	0.91	1.24	—
P1	0.86[b]	—	1.45	—	—
P2	0.96[a]	1.09[a]	1.59	—	—
P3	0.94	—	1.37	—	—
P4	0.81[a]	1.02[a]	1.52	—	—
P5	0.92[b]	—	1.45	—	—

[a] Overlap of two peaks.

[b] Peak potential.

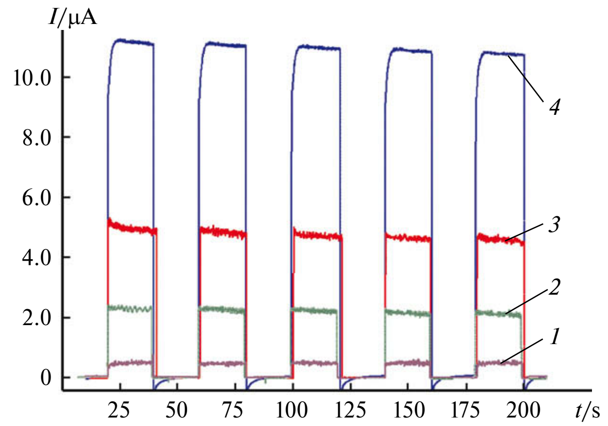

Fig. 3. The current with the LED turned off and on for devices based on binary mixtures **F1-P3** (*1*), **F2-P1** (*2*), **F1-P6** (*3*) and dyad **FP3** (*4*) (all the values are corrected for background dark current equal to 0.1 μA).

Note. Figure 3 is available in full color on the web page of the journal (http://www.link.springer.com/journal/11172).

phyrin ring from 1.03 V (**FP3**)/0.94 V (**P3**) for trifluoromethylphenyl-substituted to 0.83 V (**FP4**)/0.81 V (**P4**) for methoxyphenyl-substituted compounds. Dyad **FP2** and porphyrin **P2** "fall out" of this series, which may be due to the specific features of electron transfer kinetics in *meso*-tolyl-substituted porphyrins.

In photovoltaic cells with dyads **FP1—6** as the active layer of the working electrode, a weak dark current of about 0.1 μA appears at an applied potential of 0.1 V. Illumination of the cell with a LED leads to the appearance of an additional current, which disappears when the light is turned off. A typical example of the photogalvanic response is shown in Fig. 3. The statistical processing of the data array obtained by measuring samples with different dyads, as well as the reference system **Ref-P1** based on **P1** and fullerene derivative $\mathrm{PC_{61}BM}$,[3] most often used in photovoltaic experiments, are given in Table 2.

Processes occurring in cells based on the porphyrin-fullerene system are shown schematically in Scheme 1. After the photo-induced electron transfer from porphyrin in the excited state (**P***) to the fullerene component, a pair of charge carriers appears, namely, the porphyrin radical cation and the fullerene radical anion. The cation radical center migrates to the "photoactive material—electrolyte" interface through a series of successive redox processes involving porphyrin fragments, where oxidation of the ascorbate anion takes place with the formation of a hydrate of the cyclic form of dehydroascorbic acid,[18] while the radical anion center migrates to the "photoactive material—ITO" interface in a similar manner, where it gives away an electron to the external circuit. As a result, the oxidation of ascorbic acid accelerates under the influence of solar energy, which is experimentally registered as the appearance of additional photocurrent (compared to dark current) in the circuit. Dehydroascorbic acid can diffuse to the auxiliary electrode and undergo reduction on it, consequently acting as a mediator of electron transfer in the cell.

A comparison of measurement results for devices **Ref-P1** and **F1-P1—F6-P1** when taking into account the known performance of materials based on $\mathrm{PC_{61}BM}$ suggests that the efficiency of materials **F1-P1—F6-P1** will

Table 2. Average photocurrent density (J_{ave}) determined for the objects of study

Material	J_{ave}/μA cm^{-2}	Material	J_{ave}/μA cm^{-2}	Material	J_{ave}/μA cm^{-2}
FP1	1.6±0.1	**F1-P1**	1.8±0.3	**F2-P1**	2.1±0.2
FP2	1.2±0.1	**F1-P2**	1.5±0.1	**F3-P1**	1.0±0.1
FP3	9.8±0.9	**F1-P3**	0.4±0.1	**F4-P1**	1.0±0.1
FP4	11.4±0.6	**F1-P4**	0.2±0.01	**F5-P1**	4.6±0.1
FP5	1.5±0.1	**F1-P5**	0.2±0.1	**F6-P1**	1.1±0.1
FP6	8.2±1.0	**F1-P6**	4.8±0.2	**Ref-P1***	0.9±0.1
		F1-P7	4.8±0.5		

* **Ref-P1** is an equimolar mixture of $\mathrm{PC_{61}BM}$ and 5,10,15,20-tetraphenylporphyrin.

Scheme 1

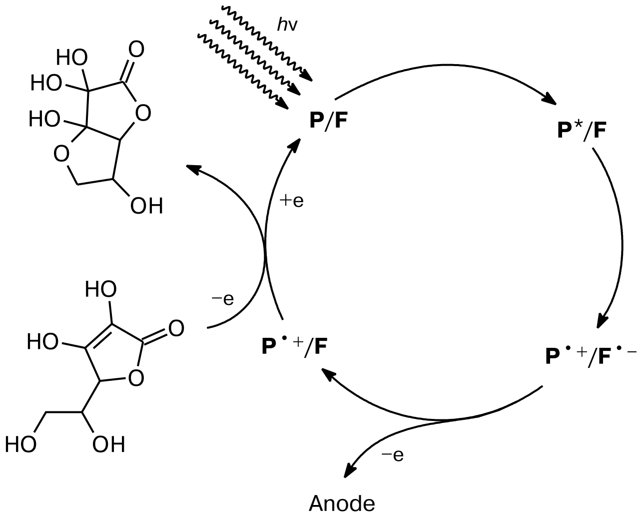

P is porphyrin, **F** is fullerene.

be comparable to the efficiency of materials based on $PC_{61}BM$.

The maximum average current density J_{ave} in the series of samples under study is demonstrated by CF_3- (**FP3**) and MeO- (**FP4**) substituted analogs of the covalently bound porphyrin-fullerene dyad **FP1** (J_{ave} = 9.8 and 11.4 μA cm^{-2} for **FP3** and **FP4**, respectively). Similarly to the work,[14] the binary mixtures of porphyrins **P3** and **P4** with pyrrolofullerene **F1** revealed considerably lower current densities (**F1-P3**, 0.2 μA cm^{-2}; **F1-P4**, 0.4 μA cm^{-2}). The photocurrent decreased on going from the dyad **FP5** to the corresponding binary mixture **F1-P5** (1.5 and 0.2 μA cm^{-2}, respectively). However, this is not a general trend. For example, similar photocurrents (1.2—1.6 μA cm^{-2}) were observed for dyads **FP1** and **FP2** and the corresponding binary mixtures **F1-P1** and **F1-P2**.

It is interesting to note that the photocurrent considerably increases when ethyl groups (**FP2**, 1.2 μA cm^{-2}) are substituted with butyl groups (**FP6**, 8.2 μA cm^{-2}) in the pyrrolofullerene fragment of the dyads. It is known that the alkyl chain length has a considerable effect on the molecular packing in *meso*-(*p*-alkoxy)aryl-substituted porphyrin films and this, in particular, leads to an increase in the exciton mean free path in the donor phase for hexyl-substituted compounds compared to ethyl-, butyl-, and octyl-substituted compounds.[19] To evaluate the effect of the alkyl chain length in donor and acceptor components of the photoactive layer on the photogalvanic characteristics of the material, we conducted a series of experiments with binary mixtures **F1-P1**—**F6-P1** containing fullerene with alkyl substituents of different lengths and the same porphyrin, and mixtures **F1-P6** and **F1-P7** containing porphyrin with different β-alkyl substituents and the same fullerene. The materials **F1-P1**—**F6-P1** revealed close photocurrent values within 1—2 μA cm^{-2}. The only exception was the material **F5-P1** based on dibutyl-substituted fulleropyrrolidine **F5** with a *cis*-configuration of the pyrrolidine fragment, for which the photocurrent was 4.6 μA cm^{-2}. Materials **F1-P6** and **F1-P7** based on tetrabutano- and octoethyl-substituted porphyrins also revealed a high photocurrent, which was equal to 4.8 μA. The high values of photocurrent demonstrated by materials **FP6**, **F5-P1**, **F1-P6**, and **F1-P7** indicate that it is possible to considerably change photogalvanic characteristics by modifying the alkyl chains in the fullerene fragment. However, based on the results of experiments with composites **F1-P1**—**F6-P1**, it is impossible to predict the substituent that will ensure the optimal morphology of the photoactive layer.

The high values of photocurrent for covalently bound dyads containing substituents with powerful σ-acceptor (CF_3) or π-donor (MeO) properties in the porphyrin core, against the background of nearly zero photocurrent in similar binary mixtures can be explained as follows. It is likely that porphyrins bearing substituents with strong electronic effects, which considerably perturb the π-system of the porphyrin core due to aggregation caused by dipole-dipole interactions, form large size domains forming a separate microphase. Consequently, there is no interpenetrating network of donor and acceptor phases in binary mixtures **F1-P3** and **F1-P4**. In contrast, in dyads **FP3** and **FP4**, the porphyrin and fullerene fragments are covalently bonded to each other, therefore, the formation of porphyrin-porphyrin aggregates leads to an automatic formation of fullerene-fullerene aggregates, resulting in the formation of two adjacent donor and acceptor phases. In the case of porphyrins **P1** and **P2**, which have a less perturbed π-system, and based on them dyads **FP1** and **FP2**, the formation of porphyrin-fullerene associates appears to successfully compete with porphyrin-porphyrin association, which leads to a similar morphology of films of homo- and heterogeneous systems.

In conclusion, pyrrolofullerene acceptors in porphyrin-fullerene photoactive materials show a photogalvanic effect comparable to that of $PC_{61}BM$ in model photovoltaic cells. A considerable increase in the photocurrent in such a system is observed in the presence of solubilizing alkyl groups in the fullerene or porphyrin component of the binary mixture, as well as in covalently bound donor-acceptor porphyrin-pyrrolofullerene dyads. An analysis of the observed photogalvanic effect shows that covalently bound porphyrin-fullerene dyads containing trifluoromethyl- methoxy-, and methyl-substituted tetraphenylporphyrin fragments are the most promising for further testing in bulk-heterojunction photovoltaic cells.

Experimental

Methanofullerene $PC_{61}BM$,[20] pyrrolofullerenes **F1—6**,[21] porphyrin-fullerene dyads **FP1—6**,[22] and porphyrins **P1—5**,[22] **P6**,[23] and **P7**[24] were synthesized following the known procedure. Commercially available acetone, propan-2-ol, and chlorobenzene were distilled before use, dichloromethane was distilled over $CaCl_2$, tetraethylammonium tetrafluoroborate (98%, Aldrich) was recrystallized from a water—propan-2-ol mixture and air-dried at 120 °C for 24 h, sodium sulfate (anhydrous, pure grade), ascorbic acid (pure grade), and acetonitrile (Kriokhrom, high purity grade) were used without prior purification.

Cyclic voltammetry. Cyclic voltammetry measurements (an Autolab PGSTAT30 potentiostat-galvanostat (EcoChemie, Netherlands)) were carried out at 25 °C in a 0.1 *M* solution of Et_4NBF_4 in MeCN in a three-electrode cell consisting of a working electrode (glassy carbon disc, 0.07 cm^2), counter electrode (platinum plate, 1 cm^2), and reference electrode (BASi MF-2062 Ag/0.1 *M* $AgNO_3$ in MeCN, calibrated with respect to the external standard of $1 \cdot 10^{-3}$ *M* ferrocene used as a pseudo-reference electrode). All potentials on voltammograms are given relative to this reference electrode, whose potential relative to the aqueous reference electrode Ag/AgCl/KCl(sat.) is +0.4 V. Nitrogen of high purity (99.999%, Lentekhgaz) was bubbled through the solutions to remove dissolved oxygen. Films for measurements were prepared directly on the electrodes by evaporating the solvent from the solution of the studied sample in CH_2Cl_2 (1 wt.%).

Preparation of photoactive electrodes. The films were formed on a substrate of indium-tin oxide deposited onto a glass plate. Before applying films of photoactive material, the surface of ITO plates was cleaned with dichloromethane, followed by ultrasonic treatment at 50 °C in acetone, distilled water, propan-2-ol, and in acetone again for 30 min for each solvent, after which the plates were air-dried at 120 °C for 5 h. The films of photoactive layer were formed by applying an aliquot (50 μL) of either a mixture prepared from equal volumes of pyrrolofullerene (0.86 mmol L^{-1}) and porphyrin (0.86 mmol L^{-1}) solutions in chlorobenzene or a porphyrin-fullerene dyad solution (0.86 mmol L^{-1}) to a rotating substrate (3500 rpm). The obtained films were air-dried at room temperature for 24 h. The working area of the active layer was limited to 1 cm^2 using a mask from a hydrophobic paraffin film.

Measurement of the photogalvanic effect. Photogalvanic measurements were performed in a three-electrode cell with a photoactive electrode acting as a working electrode (1 cm^2), a silver chloride electrode (KCl (sat.)) acting as a reference electrode, and a platinum auxiliary electrode (1 cm^2). The cell, made of optically transparent glass, with submerged electrodes was filled with supporting electrolyte (0.1 *M* aqueous Na_2SO_4) containing ascorbic acid (0.05 mol L^{-1}) used as a mediator of electron transfer and purged with argon for 20 min. The measurements were carried out with an applied potential of 0.1 V. A light emitting diode with a luminous flux at the sample location equal to 100 mW cm^{-2} and a maximum wavelength of radiation equal to 470 nm was used as the radiation source. When the LED was turned off, the potentiostat-galvanostat recorded a dark current that corresponded to the anodic oxidation of ascorbic acid. Turning on the LED resulted in a light current that was different from the dark current. The photoelectric characteristic of the objects of study was the photocurrent determined as the difference between the light and the dark currents calculated per surface area unit of the photoactive layer. A series of experiments (from six (for **F5-P1**) to 37 (for **F4-P1**)) was performed for each object of study, followed by statistical processing of the obtained data.

The studies were carried out using the equipment of the resource centers of the Research Park of St. Petersburg State University "Magnetic Resonance Research Methods", "Substance Composition Analysis Methods", "Chemistry Education Resource Center", and "Center for Innovative Technologies of Composite Nanomaterials".

This work was financially supported by the St. Petersburg State University (Grant No. 12.40.1427.2017) and the Russian Foundation for Basic Research (Project No. 18-03-00864).

References

1. Y. Huang, E. J. Kramer, A. J. Heeger, G. C. Bazan, *Chem. Rev.*, 2014, **114**, 7006.
2. S. Günes, H. Neugebauer, N. S. Sariciftci, *Chem. Rev.*, 2007, **107**, 1324.
3. M. T. Dang, L. Hirsch, G. Wantz, *Adv. Mater.*, 2011, **23**, 3597.
4. S. H. Lee, D. H. Kim, J. H. Kim, G. S. Lee, J. G. Park, *J. Phys. Chem. C*, 2009, **113**, 21915.
5. F. Tang, K. Wu, K. Duan, Y. Deng, B. Zhao, S. Tan, *Dyes Pigm.*, 2019, **160**, 79.
6. S. H. Chan, C. P. Chen, T. C. Chao, C. Ting, C. S. Lin, B. T. Ko, *Macromolecules*, 2008, **41**, 5519.
7. R. D. Kennedy, A. L. Ayzner, D. D. Wanger, C. T. Day, M. Halim, S. I. Khan, S. H. Tolbert, B. J. Schwartz, Y. Rubin, *J. Am. Chem. Soc.*, 2008, **130**, 17290.
8. W. C. Zhao, D. P. Qian, S. Q. Zhang, S. S. Li, O. Inganäs, F. Gao, *Adv. Mater.*, 2016, **28**, 4734.
9. J. E. Coughlin, Z. B. Henson, G. C. Welch, G. C. Bazan, *Acc. Chem. Res.*, 2014, **47**, 257.

10. L. Huo, S. Zhang, X. Guo, F. Xu, Y. Li, J. Hou, *Angew. Chem., Int. Ed.*, 2011, **50**, 9697.
11. T. Y. Chu, J. Lu, S. Beaupré, Y. Zhang, J. R. Pouliot, S. Wakim, J. Zhou, M. Leclerc, Z. Li, J. Ding, Y. Tao, *J. Am. Chem. Soc.*, 2011, **133**, 4250.
12. L. Dou, J. You, J. Yang, C. C. Chen, Y. He, S. Murase, T. Moriarty, K. Emery, G. Li, Y. Yang, *Nat. Photonics*, 2012, **6**, 180.
13. J. Kesters, P. Verstappen, M. Kelchtermans, L. Lutsen, D. Vanderzande, W. Maes, *Adv. Energy Mater.*, 2015, **5**, 1500218.
14. Y. Tamura, H. Saeki, J. Hashizume, Y. Okazaki, D. Kuzuhara, M. Suzuki, N. Aratani, H. Yamada, *Chem. Commun.*, 2014, **50**, 10379.
15. A. Buldum, D. H. Reneker, *Nanotechnology*, 2014, **25**, 235201.
16. A. S. Konev, A. F. Khlebnikov, O. V. Levin, D. A. Lukyanov, I. M. Zorin, *ChemSusChem*, 2016, **9**, 676.
17. M. H. Lee, J. W. Kim, C. Y. Lee, *J. Organomet. Chem.*, 2014, **761**, 20.
18. P. Karabinas, D. Jannakoudakis, *J. Electroanal. Chem.*, 1984, **160**, 159.
19. M. Kaushal, A. L. Ortiz, J. A. Kassel, N. Hall, T. D. Lee, G. Singh, M. G. Walter, *J. Mater. Chem. C*, 2016, **4**, 5602.
20. Y. Jin, J. Jee, H. Kim, S. Song, S. H. Park, J. Kim, S. W. Kang, H. Y. Woo, K. Lee, H. Suh, *Synth. Met.*, 2009, **159**, 1529.
21. A. S. Konev, A. A. Mitichkina, A. F. Khlebnikov, H. Frauendorf, *Russ. Chem. Bull.*, 2012, **61**, 863.
22. A. A. Strelnikov, D. V. Androsov, A. S. Konev, D. A. Lukyanov, A. F. Khlebnikov, A. V. Povolotskiy, K. Yamanouchi, *Tetrahedron*, 2018, **74**, 3007.
23. N. Ono, H. Kawamura, M. Bougauchi, K. Maruyama, *Tetrahedron*, 1990, **46**, 7483.
24. J. L. Sessler, A. Mozaffari, M. R. Johnson, *Org. Synth.*, 1992, **70**, 68.

Received October 22, 2018;
in revised form February 18, 2019;
accepted February 25, 2019